

Binding energy of shallow acceptors in $\text{In}_x\text{Ga}_{1-x}\text{As}/\text{GaAs}$ strained quantum wells

A. P. Roth, D. Morris, R. A. Masut,* and C. Lacelle

*Laboratory of Microstructural Sciences, Division of Physics, National Research Council,
Ottawa, Canada K1A 0R6*

J. A. Jackman

*Canada Center for Mineral and Energy Technology, Department of Energy Mines and Resources,
Ottawa, Canada K1A 0G1*

(Received 25 January 1988; revised manuscript received 31 May 1988)

The binding energy of carbon and magnesium acceptors in $\text{In}_{0.12}\text{Ga}_{0.88}\text{As}/\text{GaAs}$ strained single and multiple quantum wells is deduced from the analysis of low-temperature photoluminescence spectra of several samples with various well and barrier thicknesses. The experimental values are compared to those calculated taking into account the strain-induced valence-band splitting and anisotropy and assuming infinite potential barriers. The binding energy E_A is reduced by biaxial compressive strain and increased by spatial confinement. As a result, E_A is larger than in the unstrained bulk material only for acceptors at the center of very narrow wells ($\lesssim 50 \text{ \AA}$).

Strained quantum wells or superlattices (SL's) of several lattice mismatched semiconductors are now routinely grown. Among them, structures made of $\text{In}_x\text{Ga}_{1-x}\text{As}/\text{GaAs}$ have been studied both for their potential for devices and for their fundamental electrical and optical properties.¹⁻⁹ However, only intrinsic optical properties have been studied in detail so far, although the effects of strain and confinement which determine these properties certainly affect impurities as well.⁶ In particular, the most interesting aspect of these strained layer structures is the possibility to adjust the valence-band configuration by adjusting the strain.^{5,7,10,11} In this Rapid Communication we present experimental evidence of the effects of strain and confinement on acceptors in $\text{In}_{0.12}\text{Ga}_{0.88}\text{As}$ quantum wells. The analysis of photoluminescence spectra of a series of unintentionally doped and magnesium-doped single-quantum-well (SQW) and multiple-quantum-well (MQW) structures yields the variation of acceptor binding energy as a function of well width. The experimental values are compared to those calculated with a simple model taking into account both strain and confinement.

All the samples were grown by low-pressure metal-organic vapor-phase epitaxy. The sample parameters given in Table I are nominal values deduced from measurements of growth rate, composition, and doping concentration on thick layers. The structures were grown on a thick GaAs buffer layer ($\sim 1.5 \mu\text{m}$) except for sample 7 which was grown on a thick $\text{In}_{0.06}\text{Ga}_{0.94}\text{As}$ layer ($1.5 \mu\text{m}$). This buffer layer has the lattice constant of the unstrained alloy so that in the structure of sample 7 both the barriers (GaAs) and the wells ($\text{In}_{0.12}\text{Ga}_{0.88}\text{As}$) are under strain. In all the other samples only the wells are strained. In the undoped structures the major residual acceptor is carbon. In the doped samples the whole buffer and structure were doped under growth conditions such that the dopant concentration is slightly larger in the wells than in the barrier. Electrochemical profiles of doped layers have provided the carrier concentration, while secondary-ion-mass spectro-

scopy (SIMS) was used to obtain a precise variation of the Mg profile. The SIMS profile of sample 8 is shown in Fig. 1. The period of the structure is 17.5 nm with 7.5-nm wells and 10-nm barriers. The magnesium profile follows closely the indium one, and the Mg concentration varies by a factor of 2 between the wells and the barriers. The acceptor concentration is therefore slightly larger near the center of the wells than near the edges.

The low-temperature photoluminescence spectra were measured with samples mounted strain free in a continuous-flow liquid-helium cryostat. The sample temperature could be varied between 4.5 and 300 K. The luminescence was excited by an argon ion laser ($\lambda = 514.5 \text{ nm}$) focused on the sample surface. The detection was performed with a $\frac{3}{4}$ -m spectrometer and a cooled S1 photomultiplier with photon-counting techniques. The spectral resolution was adjusted to 0.5 meV.

The spectra of two samples having the same structural characteristics ($W=2 \text{ nm}$) but different acceptor concentrations are shown in Fig. 2. Both spectra are dominated by a strong excitonic peak (a) with a much weaker struc-

TABLE I. Structural and electrical parameters of the samples. W and B are the well and barrier thickness.

Sample	No. of periods	W/B (nm)	Doping p (cm^{-3})
1	10	2/10	undoped
2	10	2/10	10^{15}
3	10	2.5/10	5×10^{16}
4	10	3/10	undoped
5	10	5/10	10^{16}
6	10	5/5	undoped
7	10	5/5	undoped
8	10	7.5/10	10^{17}
9	SQW	7.5	undoped
10	20	10/10	undoped

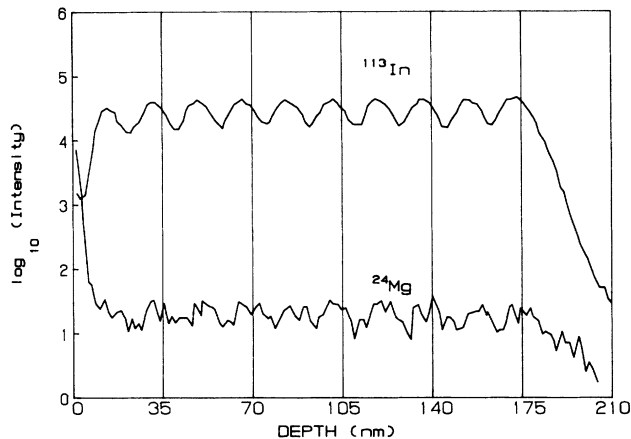


FIG. 1. SIMS profile of a magnesium-doped sample with 10 periods of 7.5-nm wells and 10-nm barriers.

ture (b) at lower energy. The spectra of Fig. 2 and those of Fig. 3 for a structure with wider wells ($W=7.5$ nm) and higher doping levels show that the weak structure becomes sharper and is well defined when the laser power is reduced or when the temperature is raised slightly in the lightly doped samples. The saturation of this emission with increasing laser power shows that it is not excitonic, and since its intensity increases with p doping it involves acceptors. Also, the peak of the emission occurs always at an energy 10 meV or more below the confined exciton peak, and must therefore involve electrons and acceptors confined in the wells or very near the interface in the barrier. Therefore, structure (b) is assigned to $(e-A^0)$ transitions between such electrons and neutral acceptors. At very low doping levels a contribution from donor-acceptor recombination is possible so that the transition energies in these samples were measured at ~ 10 K. Slightly raising temperature favors electron-neutral-acceptor $(e-A^0)$ over donor-acceptor pair recombinations. The same kind of $(e-A^0)$ transitions have been observed in $\text{Al}_x\text{Ga}_{1-x}\text{As}/\text{GaAs}$ quantum wells.^{12,13}

The effects of strain and confinement on the band structure of $\text{In}_x\text{Ga}_{1-x}\text{As}/\text{GaAs}$ quantum wells have been dis-

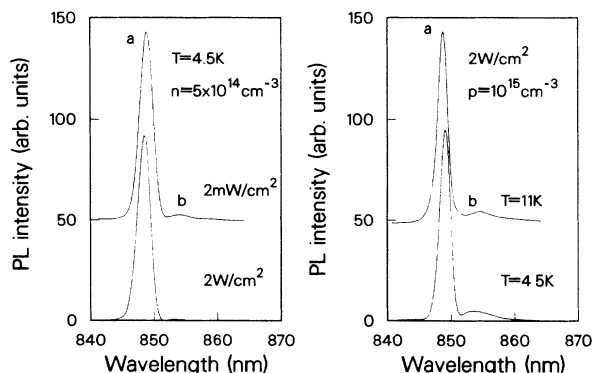


FIG. 2. Low-temperature photoluminescence (PL) spectra of two structures with 2-nm wells and 10-nm barriers and different doping levels: $n \approx 5 \times 10^{14} \text{ cm}^{-3}$ and $p \approx 10^{15} \text{ cm}^{-3}$.

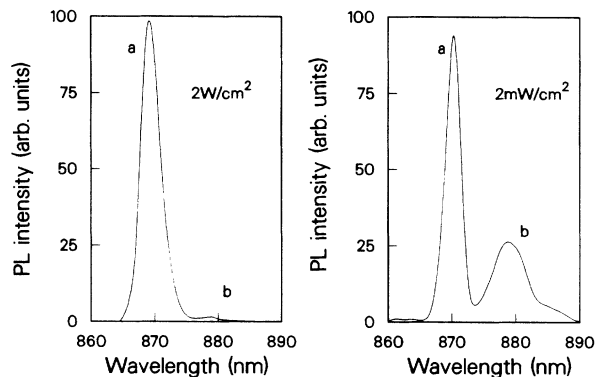


FIG. 3. Excitation power dependence of the photoluminescence spectrum for a sample with 5-nm wells, 10-nm barriers, and $p \approx 10^{16} \text{ cm}^{-3}$.

cussed in several instances.^{5,7,9-11} The ternary layers are always under compressive strain and thus the uppermost valence band in the $\text{In}_x\text{Ga}_{1-x}\text{As}$ layers is that with $m_j = \frac{3}{2}$ (heavy hole in the unstrained crystal). The uniaxial component of the strain splits the two hole bands so that in the present samples they are separated by 40 meV except for sample 7 (see Table I), which is grown on a lattice-matched buffer. In this case the strain is shared between the barriers and the wells so that the valence-band splitting in the $\text{In}_x\text{Ga}_{1-x}\text{As}$ layers is only 20 meV. Most of the experiments published so far suggest that the valence-band discontinuity in the $\text{In}_x\text{Ga}_{1-x}\text{As}/\text{GaAs}$ systems is about 30% of the band-gap difference.^{5,7,9} However, some recent experiments suggest a much larger value.⁸ The importance of this parameter for the analysis of our data resides in the fact that for a small valence-band discontinuity ($\lesssim 0.3\Delta E_g$), the $m_j = \frac{1}{2}$ holes are confined in the GaAs layers, whereas when the discontinuity is larger than the strain-induced splitting both types of holes are confined in the ternary material. Photoreflectance spectra of some of the present samples have been analyzed in detail.⁹ An excellent agreement between the calculated and experimental transitions has been achieved with a valence-band discontinuity of $0.3\Delta E_g$. In the analysis of the electron-acceptor transition energies we will therefore use this value. A precise calculation of the binding energy of acceptors in the wells as a function of strain and well width requires the solution of the Luttinger Hamiltonian including the impurity potential to which the strain Hamiltonian and confinement potential terms are added. A calculation has been performed for acceptors in $\text{Al}_x\text{Ga}_{1-x}\text{As}/\text{GaAs}$ under uniaxial compressive strain,¹³ and the predictions of this calculation are in qualitative agreement with the present experimental data once the direction of strain is reversed as in $\text{In}_x\text{Ga}_{1-x}\text{As}/\text{GaAs}$ QW's. However, the problems encountered to correctly describe the continuity of the wave function at the interface are not solved satisfactorily yet. Therefore, at this stage we prefer to make a simple numerical estimate of the acceptor binding energy. The binding energy E_A^H of acceptors in unstrained $\text{In}_x\text{Ga}_{1-x}\text{As}$ layers is smaller than the strain-induced valence-band splitting in strained layers. We measured the values of E_A^H for magnesium and

carbon acceptors in thick unstrained layers with $x=0.12$; they are (27 ± 1) meV and (24 ± 1) meV, respectively. Therefore, in a layer of $\text{In}_{0.12}\text{Ga}_{0.88}\text{As}$ strained to match the GaAs lattice constant, $E_A^s \approx 60\% \Delta E_{h-l}$, where ΔE_{h-l} is the splitting between the light- and heavy-hole bands at the Γ point. However, in strained layers the acceptor binding energy E_A^s decreases so that in first approximation $E_A^s \ll \Delta E_{h-l}$. Therefore, we calculate the binding energy of acceptor states derived from the $m_J = \frac{3}{2}$ band in strained $\text{In}_x\text{Ga}_{1-x}\text{As}$ neglecting the effects of the $m_J = \frac{1}{2}$ band.

The effect of strain on shallow impurities in bulk crystals has been discussed in the past.¹⁴ With our approximation, the problem is that of a single anisotropic band which can be treated by a variational method. The binding energy of the acceptor depends on the anisotropy factor m_{\parallel}/m_{\perp} where m_{\parallel} and m_{\perp} are the $m_J = \frac{3}{2}$ hole effective masses in the x (or y) and z directions, respectively, the latter being the growth direction. The values of the effective masses calculated using interpolated Luttinger parameters⁶ for $x=0.12$ are $m_{\parallel}=0.084$ and $m_{\perp}=0.483$. With these values, the binding energy of acceptors in strained layers is 11.5 meV, neglecting chemical shifts.

The second step in the analysis is to calculate the increase of binding energy due to confinement. However, the situation is somewhat different from that of the three-dimensional (3D) biaxially strained layer discussed above. The approximation $E_A^s \ll \Delta E_{h-l}$ should become $E_A^s \ll \Delta E_{h_1-h_2}$ and $\Delta E_{h_1-l_1}$ where $\Delta E_{h_1-h_2}$ and $\Delta E_{h_1-l_1}$ are the differences of energy between the first two heavy-hole levels and between the first heavy- and light-hole levels, respectively. In very narrow wells there is only one confined heavy-hole level but at $w=100$ Å, for instance, $\Delta E_{h_1-h_2}$ is only ~ 14 meV. On the other hand, in all samples the light holes ($m_J = \frac{1}{2}$) are confined in the GaAs barriers. Therefore, even in narrow wells where $\Delta E_{h_1-l_1}$ is small (at $w=20$ Å, $\Delta E_{h_1-l_1}=28$ meV), the two kinds of holes do not mix because they are spatially separated and the acceptor states are thus derived only from the $m_J = \frac{3}{2}$ hole states. Thus the acceptor wave function is always built from the heavy-hole states in the well, and to that extent the one-band approximation is still acceptable. However, this applies strictly to center well acceptors as the wave function of the edge acceptors depends also on the light-hole states because the overlap with these barrier states is not negligible. To study the effect of confinement, we use the infinite-barrier approximation,¹⁵ taking as the 3D binding energy the value of 11.5 meV calculated above with the corresponding effective Bohr radius. This is equivalent to considering hydrogenic acceptors with an effective mass of 0.14.

To compare these calculated acceptor binding energies to experimental data we should know the binding energy of excitons in the wells. No reliable measurement of this binding energy has been done so far. The binding energy of the exciton E_{Bx} in the well is therefore calculated using the same approximations as for the acceptors.¹⁵ The effect of strain on the binding energy is much smaller for excitons than for acceptors, since the exciton reduced mass is dominated by that of the electron which is not

affected much by strain. However, the relative binding energy increase due to confinement is more important for excitons than for acceptors, since the Bohr radius of excitons is about 3 times that of acceptors. The infinite-barrier-height model overestimates the binding-energy increase, especially when the well width is smaller than the Bohr radius, because it does not take into account the extension of the wave function in the barrier. Thus, the exciton binding energies we have calculated are overestimated. Therefore, to compare the experiments and the calculations we have subtracted the binding energy of the exciton from that of the acceptor, and we compare this difference to the difference between the excitonic photoluminescence peak and the electron-neutral-acceptor recombination since $E_A - E_{Bx} = E_x - E(e-A^0)$. E_A and E_{Bx} are the binding energies of the acceptor and the exciton, respectively, and E_x and $E(e-A^0)$ are the experimental transition energies. The calculated and experimental energy differences are plotted in Fig. 4. The error in the experimental points is about 1 meV, except for the narrower wells where the maximum of the $(e-A^0)$ structure is less well defined. Upon increasing temperature up to ≈ 40 K, the shift of the exciton peak to low energy is slower as the doping level is increased. This may be attributed to an increased contribution of acceptor bound excitons to peak (a). However, the comparison between experimental data and theoretical estimates in Fig. 4 is not very sensitive to the difference in the nature of the exciton because the difference between the binding energy of free and bound excitons (~ 3 meV for bulk $\text{In}_{0.12}\text{Ga}_{0.88}\text{As}$), although increased by confinement, still remains small.

As shown above, the concentration of magnesium acceptors is slightly larger in the wells than in the barriers. Experimental points should therefore correspond to center acceptors, especially for large wells.^{13,15} However, the contribution from recombinations with acceptors in the barrier, although indirect in real space, could become significant as the well width is reduced. It is therefore possible that in the narrower wells the weak emission

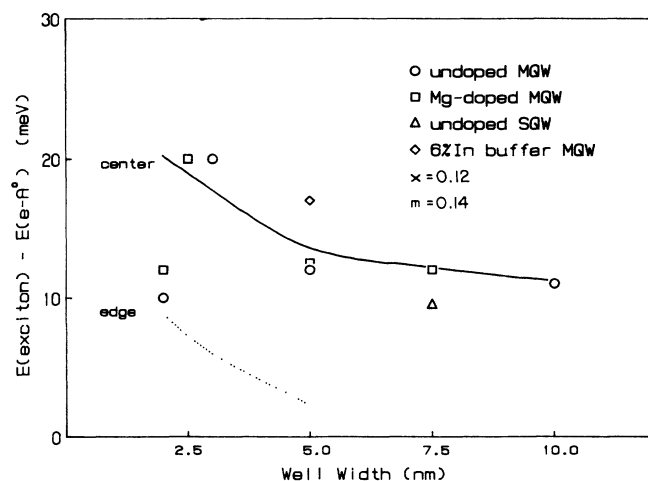


FIG. 4. Well-width dependence of the energy difference between the $e-A^0$ and excitonic recombinations measured on the PL spectra. The lines are calculated for center and edge acceptors (see text).

arises from acceptors on both sides of the interface. The agreement between the experimental points and the calculated curves is good in view of the approximations made in the present simple model. If we estimate the binding energy of excitons in the wells to increase from 6 meV for 100-Å wells to 8 meV at 20 Å,^{5,7,8} the binding energy of center acceptors deduced from the spectra increases from 18 to 28 meV. Therefore it is larger than in the unstrained bulk only for very narrow wells in contrast with what is observed for lattice-matched quantum wells.^{12,13} This is due to the effect of biaxial compressive strain which partially offsets the effects of confinement. However, the point corresponding to quantum wells grown on a matched buffer (sample 7) does not agree with the calculated curve. In this sample the compression of the wells is only 50% of that in the wells of the other samples so that the valence-band splitting is smaller. Then the acceptor state is not derived only from the $m_J = \frac{3}{2}$ state but also from the $m_J = \frac{1}{2}$ state, and the acceptor binding energy is therefore larger. A good agreement can be achieved with the present model using an effective mass of 0.16. Transport and optical experiments^{3,4} on several SL samples with $x \approx 0.2$ and well widths larger than 9 nm have shown

that the hole mass in the (x - y) plane is light with values between 0.13 and 0.17. These results suggest that the calculated mass of 0.084 is underestimated or that the $m_J = \frac{3}{2}$ band is nonparabolic even at small- k values. This should be taken into account in a more precise calculation of the acceptor binding energy. Finally, recent calculation¹⁶ based on the model used for $\text{Al}_x\text{Ga}_{1-x}\text{As}$ (Ref. 13) predicts binding energies for acceptors in $\text{In}_x\text{Ga}_{1-x}\text{As}$ quantum wells in excellent agreement with the present experimental data.

The analysis of the photoluminescence spectra of undoped and Mg-doped $\text{In}_x\text{Ga}_{1-x}\text{As}/\text{GaAs}$ strained quantum wells have shown that the binding energy of shallow acceptors in these wells is smaller than in the unstrained bulk ternary material, except in very narrow wells. This is due to the presence of strain in the wells which reduce the binding energy of acceptors because the acceptor states are mainly derived from the $m_J = \frac{3}{2}$ hole states which have a small effective mass in the x - y plane.

We are thankful to W. Trzeciakowski for his interest in this work and for many valuable comments.

*Present address: Groupe de Couches Minces (GCM), Ecole Polytechnique de Montréal, Case Postale 6079, Succursale A, Montréal, Québec, Canada H3C 3A7.

¹R. E. Zipperian and T. J. Drummond, *Electron. Lett.* **21**, 823 (1985).

²J. E. Schirber, I. J. Fritz, L. R. Dawson, and E. C. Osbourn, *Phys. Rev. B* **28**, 2229 (1983).

³I. J. Fritz, T. J. Drummond, G. C. Osbourn, J. E. Schirber, and E. D. Jones, *Appl. Phys. Lett.* **48**, 1678 (1986).

⁴E. D. Jones, H. Ackermann, J. E. Schirber, T. J. Drummond, L. R. Dawson, and I. J. Fritz, *Solid State Commun.* **55**, 525 (1985).

⁵J. Y. Marzin, M. N. Charasse, and B. Sermage, *Phys. Rev. B* **31**, 8298 (1985).

⁶A. P. Roth, R. A. Masut, M. A. Sacilotti, P. J. D'Arcy, Y. LePage, G. I. Sproule, and D. F. Mitchell, *Superlatt. Microstruct.* **2**, 507 (1986).

⁷D. Ji, D. Hwang, U. K. Reddy, T. S. Henderson, R. Houdré, and H. Morkoç, *J. Appl. Phys.* **62**, 3366 (1987).

⁸J. Menéndez, A. Pinczuk, D. J. Werder, S. K. Sputz, R. C. Miller, D. L. Sivco, and A. Y. Cho, *Phys. Rev. B* **36**, 8165 (1987).

⁹S. H. Pan, H. Shen, Z. Hang, F. H. Pollak, W. Zhuang, Q. Xu, A. P. Roth, R. A. Masut, C. Lacelle, and D. Morris, *Phys. Rev. B* **38**, 3375 (1988).

¹⁰E. P. O'Reilly and G. P. Witchlow, *Solid State Commun.* **62**, 653 (1987).

¹¹J. Y. Marzin, in *Heterostructures and Semiconductor Superlattices*, edited by G. Allan, G. Bastard, N. Boccara, M. Lannoo, and M. Voos (Springer-Verlag, Berlin, 1986), p. 161.

¹²R. C. Miler, A. C. Gossard, W. T. Tsang, and O. Munteanu, *Phys. Rev. B* **25**, 3871 (1982).

¹³W. T. Masselink, Y. C. Chang, and H. Morkoç, *Phys. Rev. B* **32**, 5190 (1985).

¹⁴G. L. Bir and G. E. Pikus, *Symmetry and Strain Induced Effects in Semiconductors* (Wiley, New York, 1974).

¹⁵G. Bastard, *Phys. Rev. B* **24**, 4714 (1981).

¹⁶Y. C. Chang, *Physica* **146B**, 137 (1987).